JOURNAL OF MATERIALS SCIENCE 16 (1981) 1527–1532

Microstructure in the weld region in seam welded and resistance welded Zircaloy 4 tubing

R. A. BORDONI,* A. M. OLMEDO†
Departamento de Combustibles Nucleares, Departamento de Química de Reactores,† Comisión Nacional de Energía Atómica, Buenos Aires, Argentina*

The microstructure of tungsten inert gas (TIG)-arc welding and resistance welding in Zircaloy 4 tubing is described in relation to the phases present. Differences in microstructure between the weld zone and base tubing are discussed in terms of the phase transformations that take place during the very different thermal cycles occurring in both processes and a comparison between them is made. A feature of the weld region is the presence of a coarse grained Widmanstätten structure in the TIG welding while a martensitic-type structure or very fine Widmanstätten structure is present in resistance welding.

1. Introduction

The low absorption cross sections of Zircaloys for thermal neutrons together with their excellent corrosion resistance, relatively good strength up to moderately high temperatures and their high degree of stability under radiation have made them valuable materials for fuel cladding in high-pressure water reactors (PWR). Zircaloy 4* has shown smaller hydrogen pick-up fraction during corrosion than Zircaloy 2 so it has therefore become the standard alloy for the PWR.

An important factor determining the properties of Zircaloys is their microstructure. This is affected by heat treatment and cold work. The fracture stress and ductility of zirconium increased with decreasing grain size [1]. Zircaloys owe their good mechanical properties to a large extent to their α-grain size but the welding and brazing processes used to attach some parts to fuel sheathing such as end plugs and bearing pads modify these properties.

Zirconium has two allotropic modifications. The α-form is close-packed hexagonal in structure and is stable up to approximately 862° C. The β-form, which is stable up to approximately 862° C, the melting point, is body-centred cubic in structure. The alloying elements added to form Zircaloys modify these temperatures. In Zircaloys the α-phase is stable up to about 825° C, a two phase $\alpha + \beta$ field extends from there up to about 975° C, and the β-phase is stable above this temperature.

During the welding of these alloys, the weldment is locally heated above the β-phase region and is cooled over a range of cooling rates; these heating and cooling cycles induce different phase transformations so that the resulting microstructures are likely to be complex in nature. Cooling after welding can result in a number of possible metallurgical conditions. On cooling from the β-phase field at moderate rates (oil quenching to furnace cooling) Zircaloys transform to give a Widmanstätten type structure; increasing the cooling rate produces finer Widmanstätten plates and quenched martensitic structures [2–4].

Two processes commonly used to attach different parts to the fuel sheathing are tungsten inert gas (TIG)-arc welding and resistance welding processes. Considering their cooling rates these processes can be divided:

*Typical composition of Zircaloy 4. Sn: 1.20–1.70 wt%; Fe: 0.18–0.24 wt%; Cr: 0.07–0.13 wt%; O: 1600 ppm (max.); balance: zirconium plus impurities.

0022–2461/81/061527–06$02.60/0

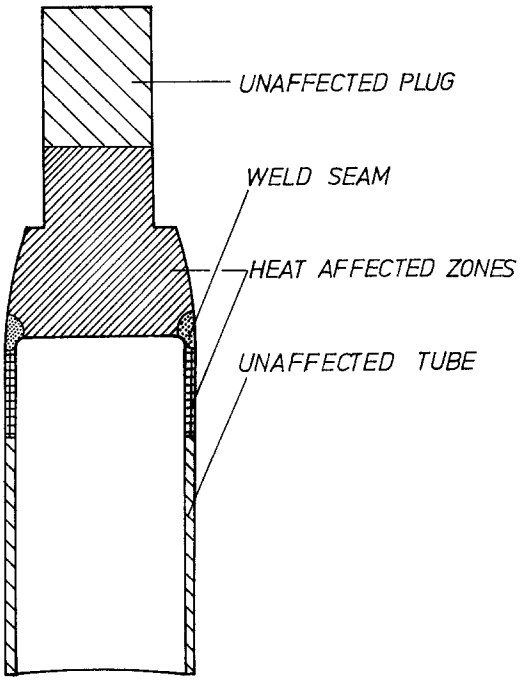

Figure 1 Schematic representation of longitudinal section through an inert gas-arc welded specimen.

(a) With resistance welding there is very rapid heating and cooling; the whole joining process takes place in less than a second and produces heating and cooling rates of the order of 10^3 ° C sec^{-1} calculated between the fusion temperature and 500° C, approximately [5].

(b) With TIG welding there is a less rapid heating and cooling; the heating and cooling rates are in the range 10 to 10^2 ° C sec^{-1}.

As there are both thermal and deformation cycles occurring during the welding operation, when either a restrained end plug or bearing pad is fitted, it is important to understand the precise nature of the phase transformations that can take place.

The purpose of this work has been to characterize the different microstructures present in Zircaloy 4 produced by the two welding processes. The fundamentals of both processes as well as their advantages and disadvantages have already been discussed in the literature [6–8].

2. Materials and experimental methods

The materials examined were the end closure plugs and bearing pads welded to canning tubes by the inert gas arc-welding process (TIG) and resistance projection welding process, respectively. All material used was Zircaloy 4 of nuclear grade. The samples were welded within specifications and different tests (such as corrosion test, burst test) commonly used in these type of welds were made. Microscopical examination showed that the welds were free from defects such as voids, porosity or cracks.

The specimens were prepared for metallographic examination by mechanically polishing them on progressively finer emergy papers, finishing on 600-grit paper. This was followed by chemical polishing using a solution H_2O:HNO_3:HF (50:47:3 vol%). Different observations in the base metal, heat affected zone and fusion zone of the welds were made using bright-field, polarized illumination and scanning electron microscopy (SEM).

Figure 2 Micrograph showing the fusion zone and part of the HAZ of a TIG welded Zircaloy 4 end plug. Normal illumination (× 50).

Figure 3 Microstructure of part of the HAZ in the end plug. Polarized illumination (× 54).

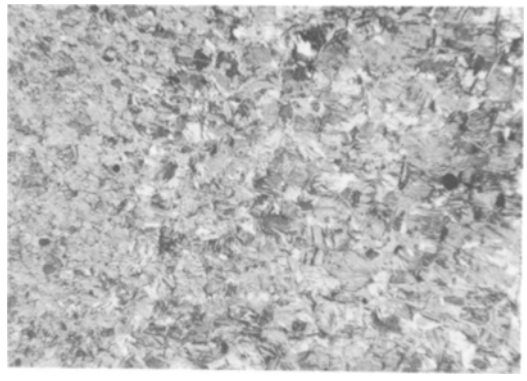

Figure 5 Microstructure corresponding to part of the HAZ in the end plug where primary islands of α-matrix and Widmanstätten structure are shown. Polarized illumination (× 48).

3. Results and discussion

3.1. Inert gas arc welding

Inert gas arc welding with argon is a process used to weld end plugs into fuel rods of nuclear reactors. This was the first process commonly used for this type of weld but now resistance welding has been developed as another process for end plug welding. Magnetic or pneumatic techniques are used for pressing the end plugs [6, 9–11].

Fig. 1 illustrates schematically a longitudinal section through a circumferential TIG welded end plug. The samples showed the following zones:

(i) weld zone;
(ii) heat affected zone (HAZ);
(iii) unaffected tube;
(iv) unaffected plug.

The weld seam contains coarse transformed β-grains and acicular α-needles representative of the actual melting of Zircaloy, Fig. 2. In a section immediately adjacent to the weld (part of the end plug and the tube) there are zones in which the temperature was raised into the β-range but not to the melting point, Fig. 3. A typical Widmanstätten structure of this part of the HAZ is shown in Fig. 4. This structure persisted into the fused region, the main difference being an increase in grain size together with the presence of some fine acicular α-grains. In the intercritical HAZ (α + β field) there is a region on the tube and on the end plug where the structure consisted of primary islands of α-matrix together with acicular α resulting from transformed β-phase (Fig. 5). Fig. 6 is a view of this zone in the end plug showing grain-boundary nucleation of the α-phase. Finally there is a region of the HAZ where the temperature did not exceed the transformation temperature, but was sufficiently high to cause recrystallization and growth of the α-grains, Fig. 7. The unaffected tube structure is characterized by α-grains showing

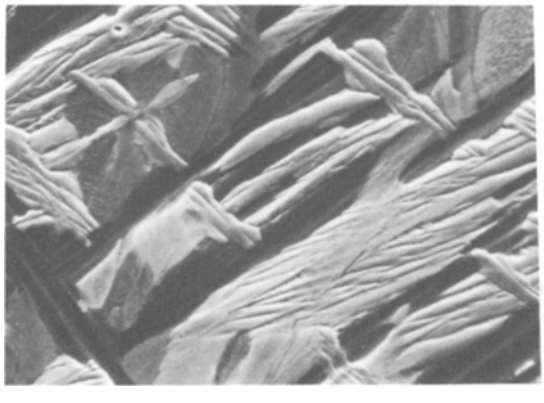

Figure 4 Typical Widmanstätten structure corresponding to the HAZ. SEM micrograph (× 720).

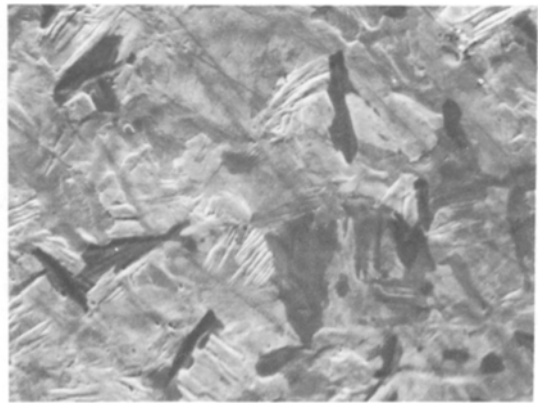

Figure 6 SEM micrograph showing grain boundary nucleation of the α-phase (× 620).

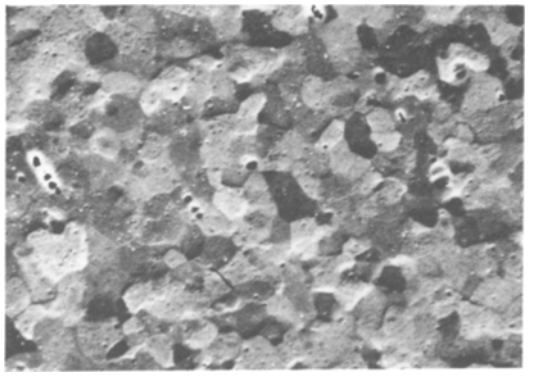

Figure 7 SEM micrograph corresponding to the part of the tube where recrystallization and growth of α-grains takes place. Specimen heavily etched (× 820).

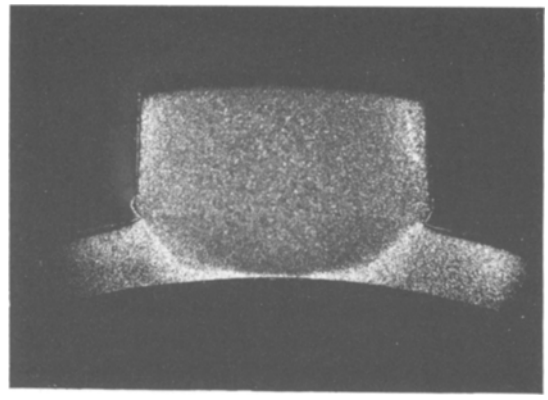

Figure 9 Resistance welded joint between a bearing pad and a sheath. Polarized illumination (× 18).

some preferred elongation due to plastic deformation during fabrication of Zircaloy fuel sheathing, while the unaffected plug has an equiaxial structure of α-grains, Fig. 8.

The weld seam and part of the HAZ which attained a temperature in the β and $\alpha + \beta$ range had a Widmanstätten structure as has already been mentioned. This structure is caused by a relatively slow cooling rate during the TIG operation. In this case the purity of the shielding gases must be controlled to ensure corrosion resistant weldments [12]. The Widmanstätten plates expand by edge growth and thicken with rejection of alloying elements. Second phase particles and β-grain boundaries nucleate α-plates; the diffusion of alloying elements (Fe and Cr) control the growth rates of these plates [2]. This behaviour resembles the diffusional growth mechanism of Widmanstätten ferrite plates from austenite proposed by Aaronson and co-workers [13, 14] in which the growth control is produced through the diffusion of carbon in austenite.

The importance of cooling rate in Zircaloy 4 is confirmed by the findings that the microstructure can change gradually with the variation of cooling rate [2–4] and this microstructural information is very closely related to its mechanical properties [15].

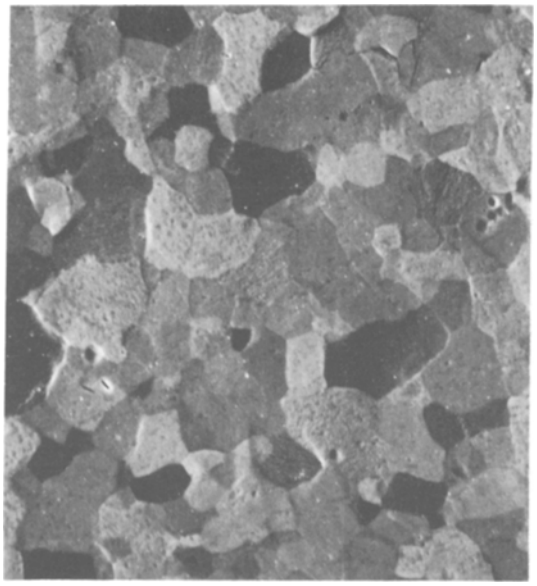

Figure 8 SEM micrograph showing the original equiaxial structure of the end plug (× 650).

3.2. Resistance welding

The high electrical and thermal resistivity of Zircaloys make them suitable for this type of welding process. One important feature of this process is that it can be performed under any gas

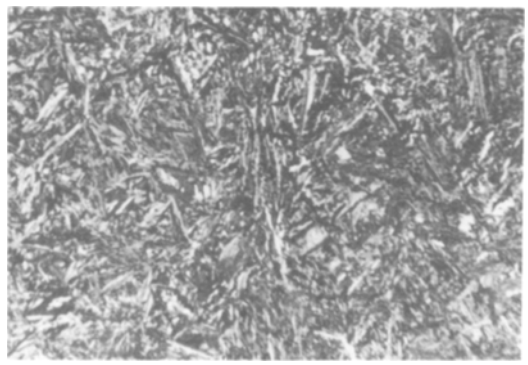

Figure 10 Microstructure of the central region of the tube corresponding to part of the HAZ of the weld. Polarized illumination (× 435).

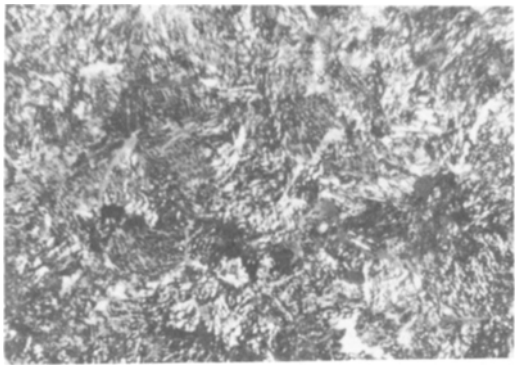

Figure 11 Microstructure of the heat affected zone of the bearing pad. Polarized illumination (× 450).

pressure, or even in air, and because the heating and cooling times are extremely short the HAZ is very small. Fig. 9 shows a resistance projection welding between a bearing pad and a clad. It was possible to identify the following zones in the weld after a suitable metallographic preparation.

(i) weld zone;
(ii) heat affected zone (HAZ);
(iii) unaffected base material.

Figs 10 to 12 indicate the microstructure of the different zones. Both the weld and the narrow HAZ are similar in that the microstructure consists of transformed β-phase. No fusion zone can be seen in Fig. 13 where there is a change in morphology on both sides of the weld line. In Fig. 14 these zones alternate with the fusion zones noticeable by the continuous morphology and the disappearance of the weld line. As it has been mentioned in a previous work [16] electron probe microanalysis indicated no segregation of iron,

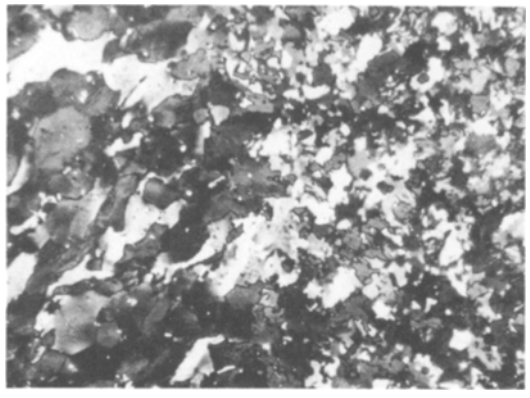

Figure 12 Transition zone between the HAZ and the tube. Polarized illumination (× 435).

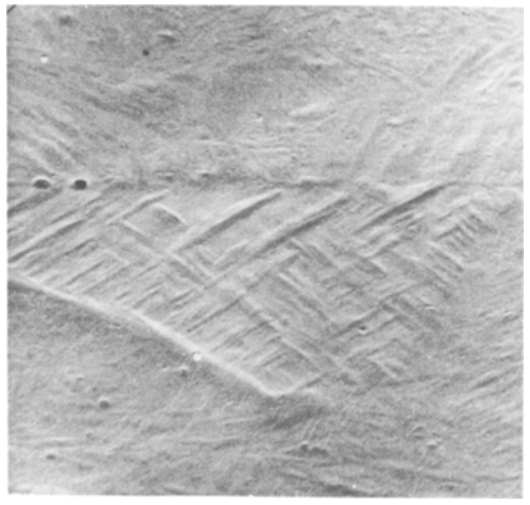

Figure 13 SEM micrograph of the interface joint showing lack of fusion. Specimen heavily etched (× 4100).

chromium and tin in the welded zone although the hardness values were higher than those of the unaffected base material. The fine acicular structure evident in Figs 10 and 11 is similar to the martensites reported by Holt [2, 3] who used cooling rates of $2.10^{3\circ}$ C sec^{-1}. Bodmer *et al.* [17] have also indicated that martensite can be formed at these high cooling rates without appreciable segregation of alloy elements occurring. The other consequence of the rapid heating and cooling is that absorption (especially of nitrogen) is kept to a minimum and, hence, good corrosion properties are produced in the weldments [9]. This is also confirmed by our experimental results.

Figure 14 SEM micrograph of the interface joint showing regions where fusion has taken place and regions where it has not. Specimen heavily etched (× 1165).

4. Conclusions

The microstructure of the weld region of TIG welded Zircaloy 4 tubing is significantly different from that of the non-welded base material. The weld seam presented a columnar β-grain representative of fusion and acicular α-needles. The HAZ possessed an intermediate grain size between that of the weld seam and the base material and may be divided into three different zones characterized by the maximum temperature obtained in each zone.

(a) Maximum temperature in the β field.

(b) Maximum temperature in the $\alpha + \beta$ field.

(c) Maximum temperature did not exceed the transformation temperature but was sufficiently high to cause recrystallization and growth of the α-grains.

In the case of resistance welded Zircaloy 4 the joint between the two surfaces can be produced without significant fusion. The HAZ is very narrow and consists principally of a martensitic-type structure or a very fine Widmanstätten structure. This very fine microstructure is due to the very rapid heating and cooling cycles.

The different microstructures of the weld region can be explained in terms of the very different thermal cycles that are produced in both processes. From the microstructural point of view, the resistance welding process, due to the rapid welding cycle, has the following advantage when compared with the TIG processes:

(i) smaller size of the HAZ;

(ii) smaller grain size;

(iii) smaller probability of contamination by impurities;

(iv) a possibility of a more homogeneous distribution of second phase particles.

Acknowledgements

The authors are indebted to Mr. J. M. Falcone, the personnel of the Metallography and Special Techniques Division of Materials Development, Comisión Nacional de Energía Atómica, and the Scanning Electron Microscopy Laboratory of the Instituto de Neurobiología for their technical assistance.

References

1. R. A. HOLT, W. EVANS and B. A. CHEADIE, Proceedings of the 4th International Conference on Materials Technology, Caracas, Venezuela, June 1975, p. 329.
2. R. A. HOLT, *J. Nuclear Mater.* **35** (1970) 322.
3. *Idem, ibid.* **47** (1973) 262.
4. O. T. WIO and K. TANGRI, *ibid.* **79** (1979) 82.
5. J. A. GREENWOOD, *Brit. Weld. J.* **8** (1961) 316.
6. J. J. VAGI and D. C. MARTIN, *Weld. J.* **39** (1960) 443S.
7. L. MILLS, *ibid.* **40** (1961) 141.
8. G. SCHNEIDER, *Kerntechnik* **11** (1969) 18.
9. K. T. BATES, Atomic Energy Canada Ltd. Report number 2814, October, 1966.
10. H. W. SCHUELER, *Weld. J.* **47** (1968) 638.
11. S. de BURBURE, *ibid.* **57** (1978) 23.
12. H. STEHLE, W. KADIN and R. MANZEL, *Nuclear Eng. and Design* **33** (1975) 155.
13. K. R. KINSMAN, E. EICHEN and H. I. AARONSON, *Metall. Trans. (A)* **6** (1975) 303.
14. J. M. RIGSBEE and H. I. AARONSON, *Acta Met.* **27** (1979) 365.
15. E. BAROCH, Proceedings of a Study Group Meeting Organized by the International Atomic Energy Agency, Grenoble, France, September, 1972 (IAEA, Vienna, 1973) 219.
16. A. M. OLMEDO, *J. Mater. Sci.* **15** (1980) 1050.
17. E. BODMER, J. J. CHENE, R. O. ERIKSON and R. FERRARINI, Proceedings of the 3rd UN International Conference on the Peaceful Uses of Atomic Energy, Geneva, September, 1964 (United Nations Publications, New York, 1965) Vol. 9, p. 173.

Received 7 July and accepted 17 October 1980.